

Ligand Evolution on Trigonal Bipyramidal Boron Imidazolate Cages for Enhanced Optical Limiting

Jun-Qiang Chen,^{1,2} Hai-Xia Zhang,^{1*} Zhi-Run Wang,^{1,2} Qin-Long Hong,¹ and Jian Zhang^{1*}

^a State Key Laboratory of Structural Chemistry, Fujian Institute of Research on the Structure of Matter, Chinese Academy of Sciences, Fuzhou, Fujian 350002, P. R. China

^b University of Chinese Academy of Sciences, Chinese Academy of Sciences, Beijing 100049, P. R. China

Email: zhanghaixia@fjirsm.ac.cn; zhj@fjirsm.ac.cn.

Content

1. Synthesis of BIFs.....	2
1. Detailed Structure Information for BIFs	3
2. The PXRD Analyses for BIFs	11
3. The UV-Vis Spectra of BIFs	14
4. The NLO Property	17
5. The TGA curve of BIFs.....	20
6. Crystallography Data	21
7. PDMS film forming method and Test methods for third-order NLO.....	23

1. Synthesis of BIFs

Synthesis of BIF-136 :

KBH(bim)₃ (0.055 g), 5-tert-Butylisophthalic Acid (0.032 g) and NiCl₂·6H₂O (0.032 g) in a distilled water (H₂O, 1 ml)/N,N-Dimethylacetamide (DMA, 2 ml)/ethanol (2 ml) solution were placed in a 20 ml vial. The sample was heated at 80°C for 5 days, and then cooled to room-temperature. After washed by ethanol and H₂O, the yellow crystals were obtained.

Synthesis of BIF-137 :

KBH(bim)₃ (0.043 g), 4,4'-Oxybisbenzoic acid (0.034 g) and NiCl₂·6H₂O (0.042 g) in a dimethyl sulfoxide (DMSO, 1 ml)/N,N-Dimethylformamide (DMF, 2 ml)/1-Butanol (2 ml) solution were placed in a 20 ml vial. The sample was heated at 80°C for 13 days, and then cooled to room-temperature. After washed by DMF and ethanol, the yellow crystals were obtained.

Synthesis of BIF-138 :

KBH(bim)₃ (0.042 g) and NiCl₂·6H₂O (0.036 g) in a dimethyl sulfoxide (DMSO, 1ml)/N,N-Dimethylacetamide (DMA, 2 ml)/1-Butanol (2 ml) solution were placed in a 20 ml vial. The sample was heated at 80°C for 3 days, and then cooled to room-temperature. After washed by DMSO and propan-2-ol (IPA), the purple crystals were obtained.

Synthesis of BIF-139 :

KBH(bim)₃ (0.043 g), 3,3'-Dithiodipropionic acid (0.030 g) and NiCl₂·6H₂O (0.032g) in a distilled water (H₂O, 1ml)/N,N-Dimethylacetamide (DMA, 2 ml)/ethanol (2 ml) solution were placed in a 20 ml vial. The sample was heated at 80°C for 8 days, and then cooled to room-temperature. After washed by ethanol, the yellow crystals were obtained.

Synthesis of BIF-140 :

KBH(bim)₃ (0.042 g) and NiCl₂·6H₂O (0.036 g) in a dimethyl sulfoxide (DMSO, 2 ml)/ N,N-Dimethylformamide (DMF, 1 ml)/ propan-2-ol (2 ml) solution were placed in a 20 ml vial. The sample was heated at 80°C for 3 days, and then cooled to room-temperature. After washed by DMSO and acetonitrile, the purple crystals were obtained.

Synthesis of BIF-141 :

KBH(bim)₃ (0.042 g), thioctic acid (0.042 g) and NiCl₂·6H₂O (0.040 g) in a distilled water (H₂O, 1 ml)/ N,N-Dimethylethanolamine (DMEA, 2 ml)/1-Butanol (2 ml) solution were placed in a 20 ml vial. The sample was heated at 80°C for 7 days, and then cooled to room-temperature. After washed by propan-2-ol, the yellow crystals were obtained.

2. Detailed Structure Information for BIFs

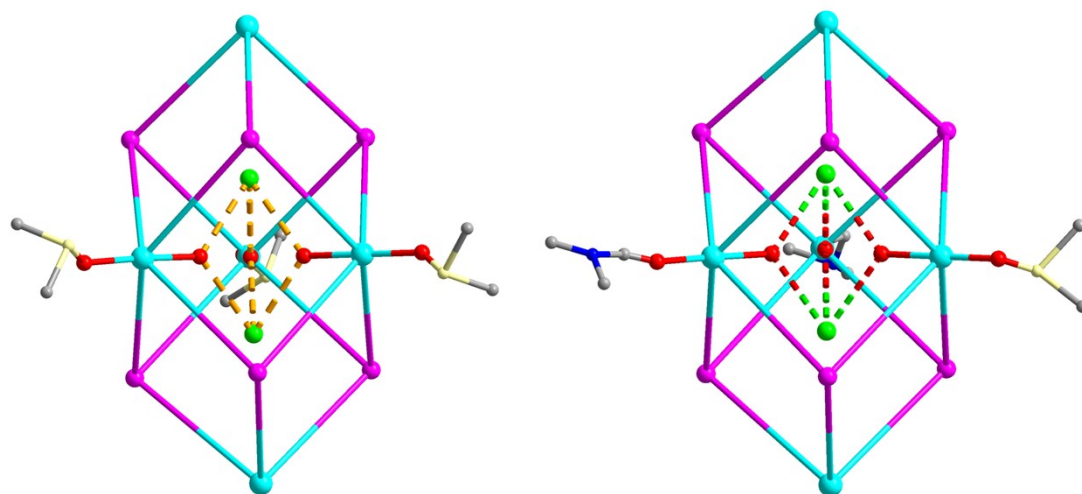


Figure S1. Trigonal bipyramidal cages with different end groups in BIF-138 (left) and BIF-140 (right).

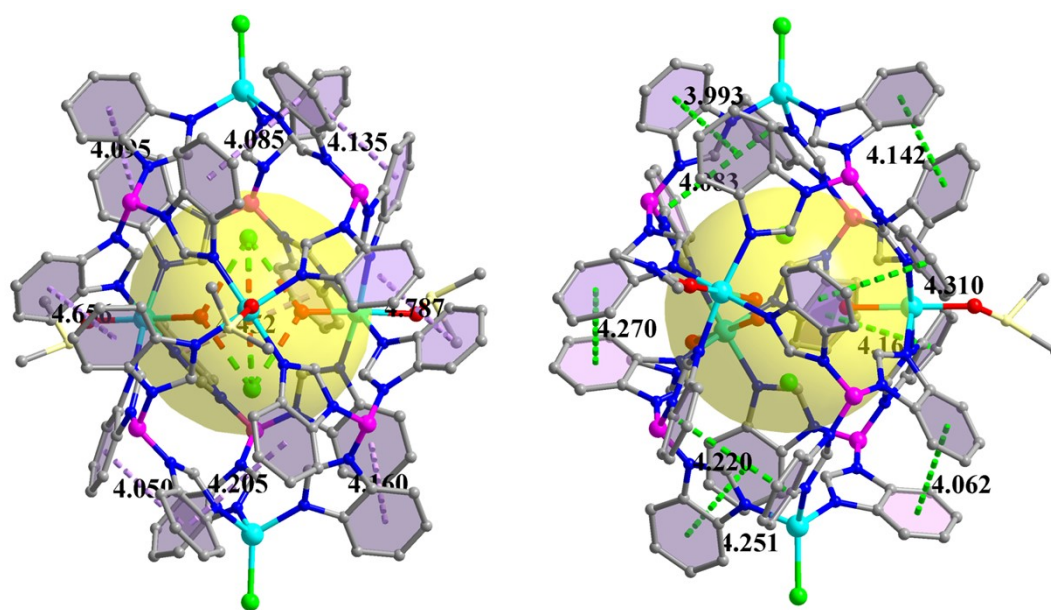


Figure S2. $\pi \cdots \pi$ interaction in BIF-138 (left) and BIF-140 (right).

(unit : Å)

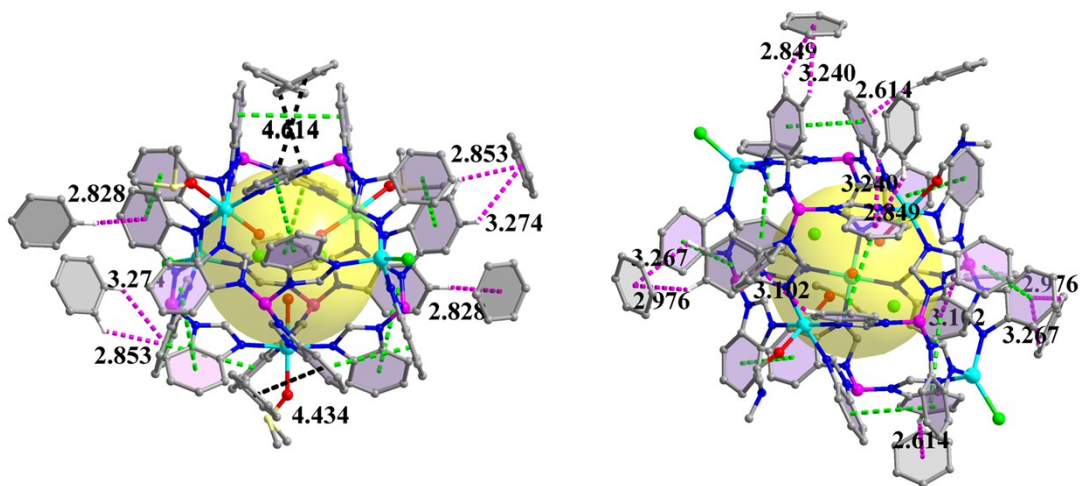


Figure S3. $\pi \cdots \pi$ interaction between neighboring molecules of BIF-138 (left) and BIF-140 (right). (unit : Å).

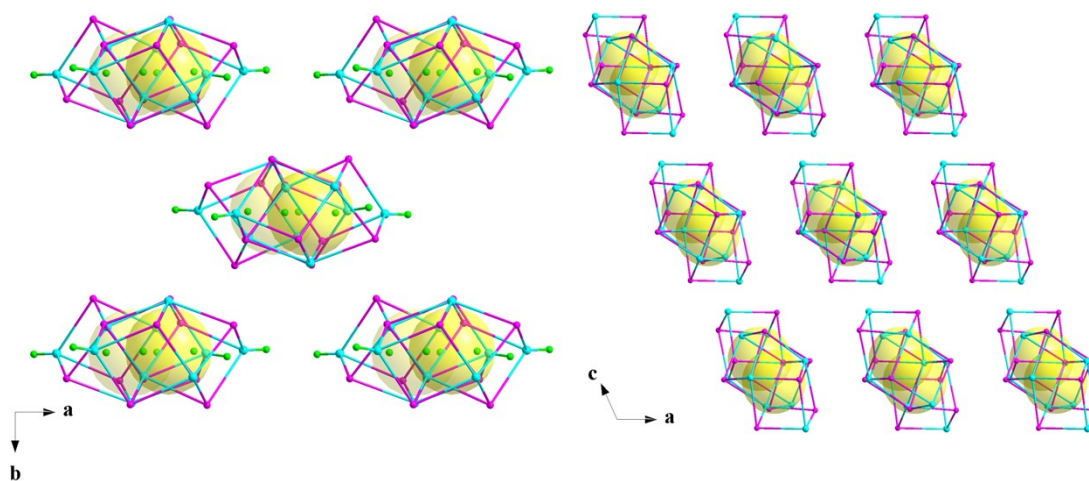


Figure S4. Stacking of BIF-138 (left) and BIF-140 (right).

The accessible free volume of BIF-138 is 24.5% as calculated by the PLATON program, and BIF-140 is 19.0%.

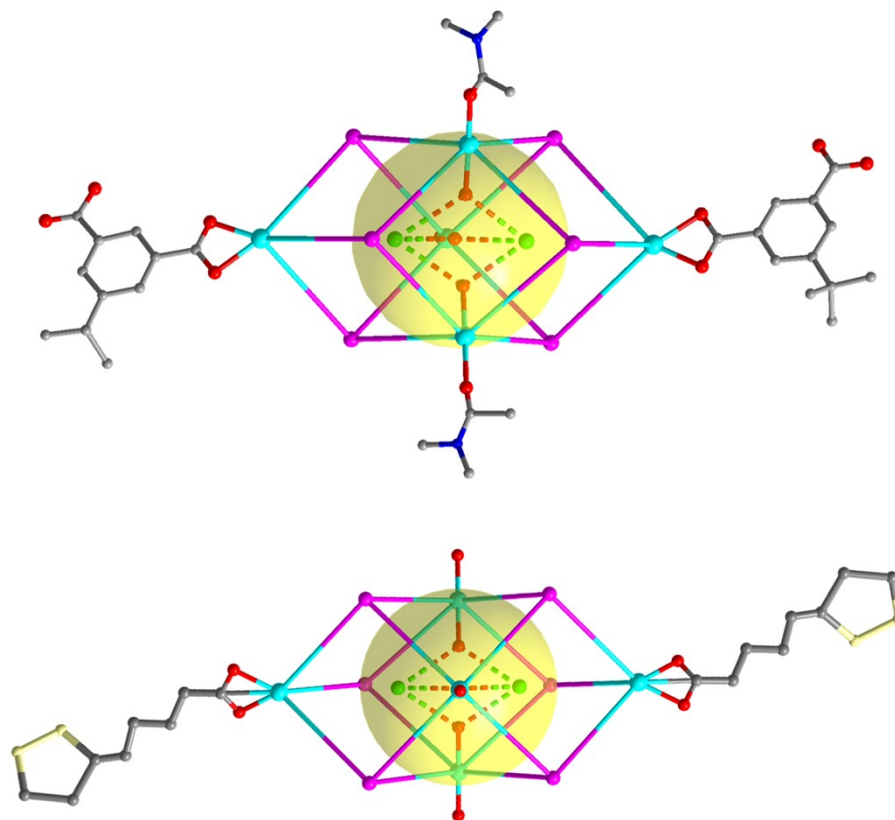


Figure S5. Structure diagram of BIF-136 (up) and BIF-141 (down).

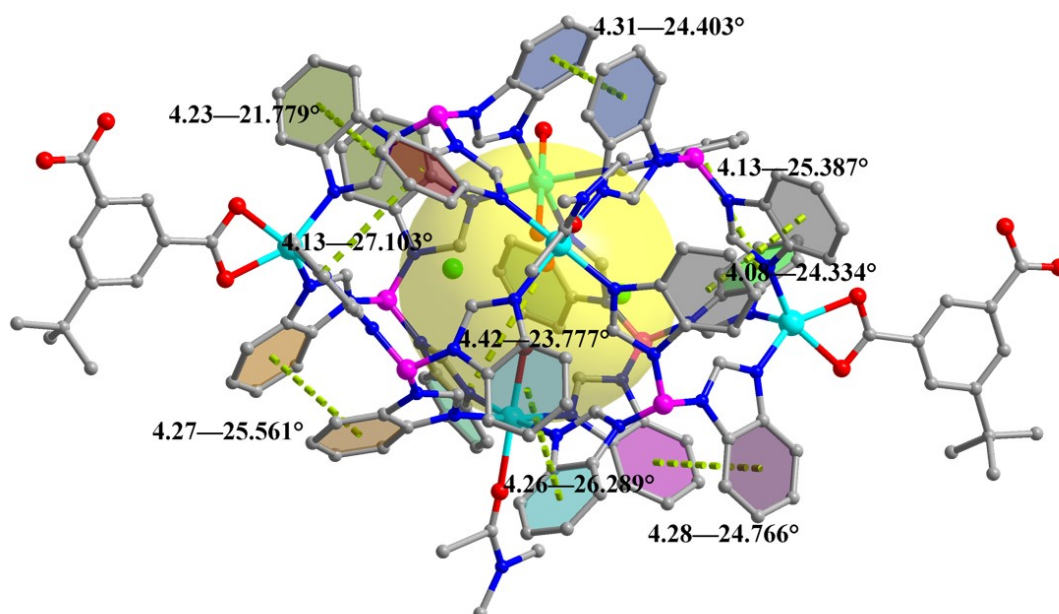


Figure S6. Intramolecular $\pi \cdots \pi$ interaction and dihedral angle in BIF-136. (unit : Å)

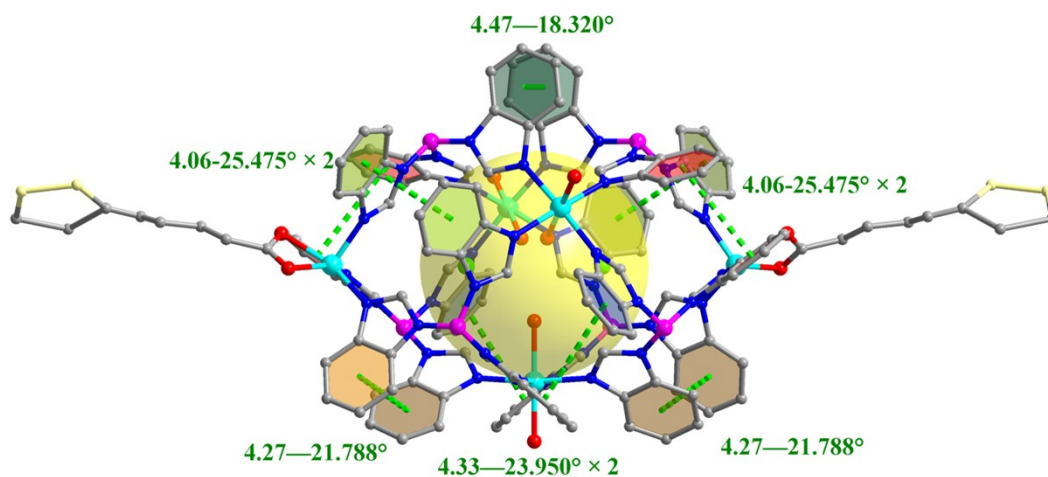


Figure S7. Intramolecular $\pi \cdots \pi$ interaction and dihedral angle in BIF-141. (unit : Å)

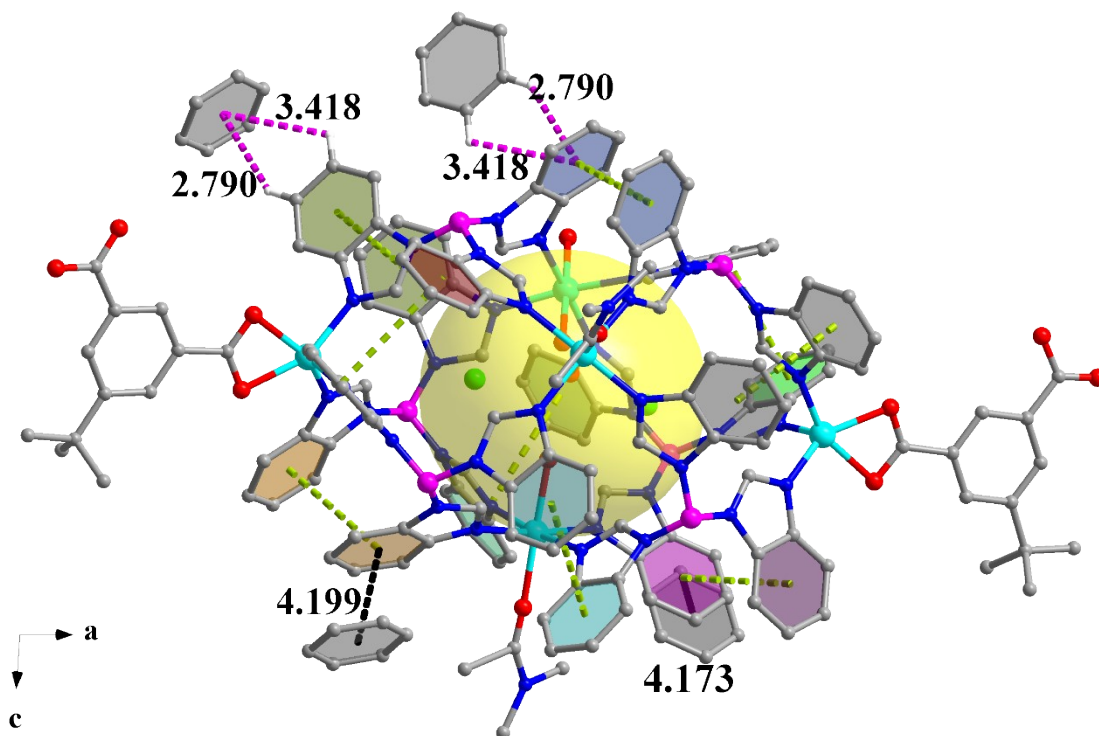


Figure S8. Intermolecular $\pi \cdots \pi$ interaction in BIF-136. (unit : Å).

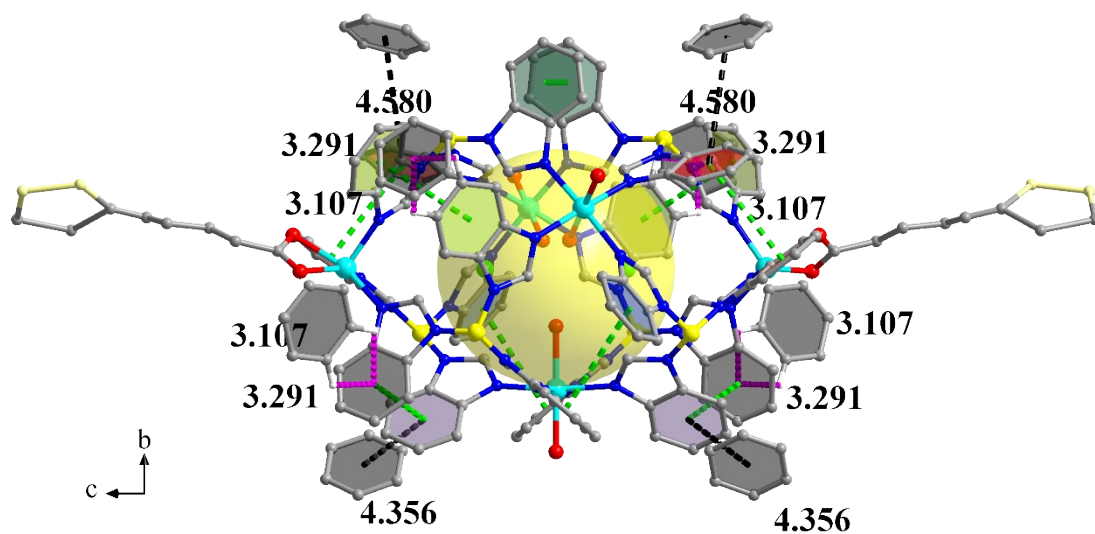


Figure S9. Intermolecular $\pi \cdots \pi$ interaction in BIF-141. (unit : Å).

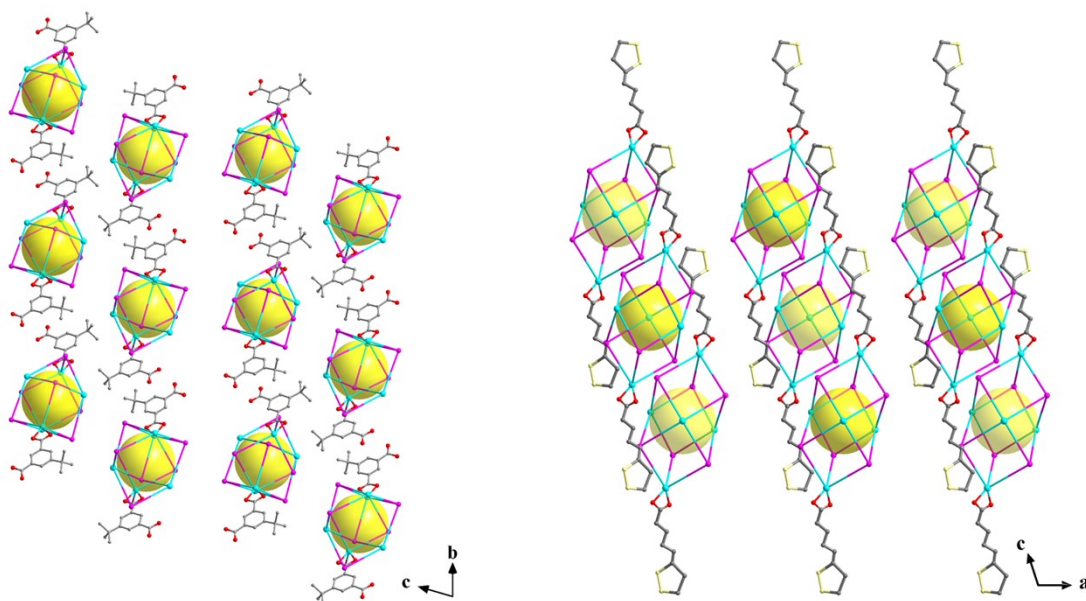


Figure S10. Stacking of BIF-136 (left) and BIF-141 (right).

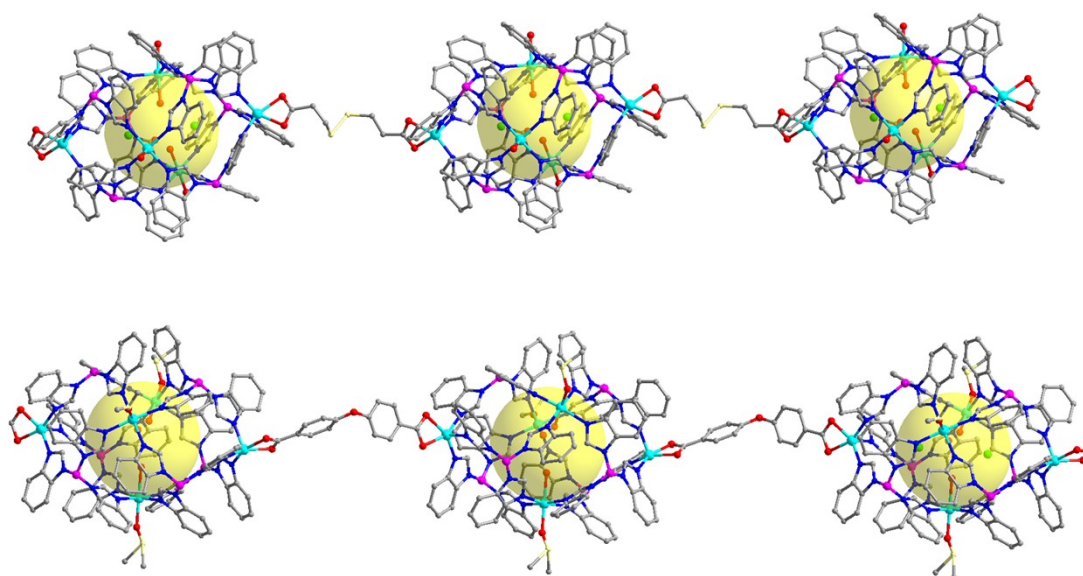


Figure S11. Structures of BIF-139 (up) and BIF-137 (down).

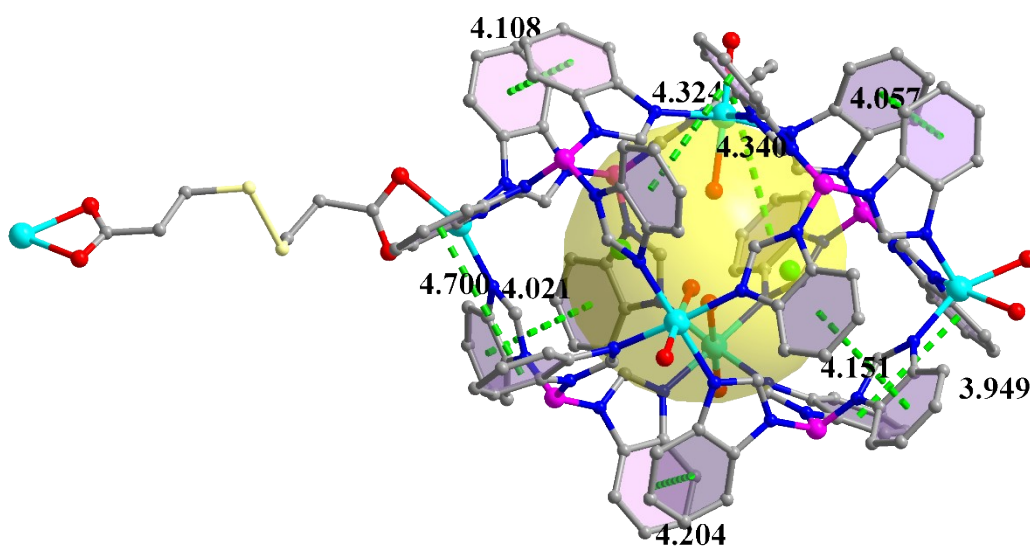


Figure S12. Intramolecular $\pi \cdots \pi$ interaction in BIF-139. (unit : Å).

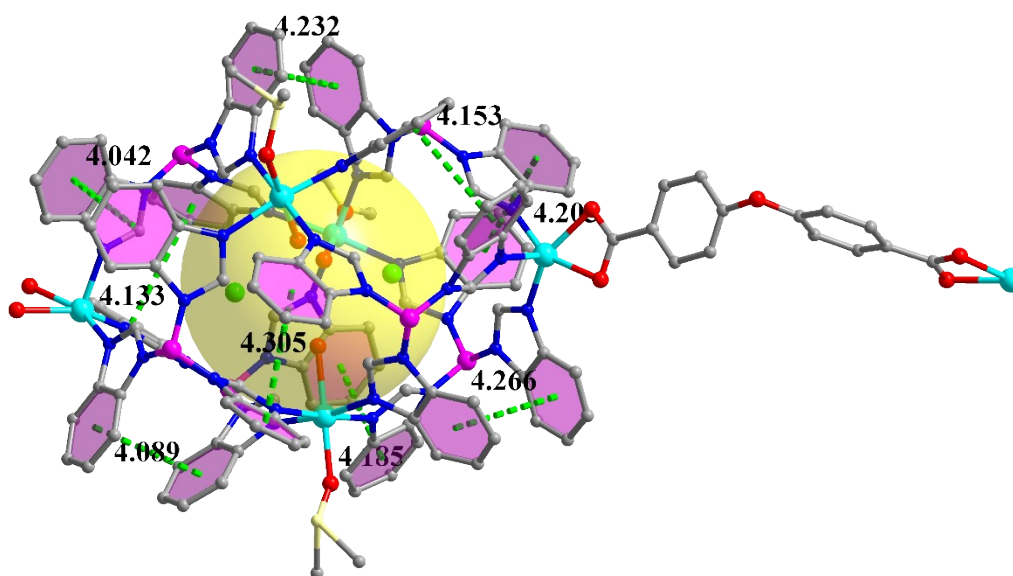


Figure S13. Intramolecular $\pi \cdots \pi$ interaction in BIF-137. (unit : Å).

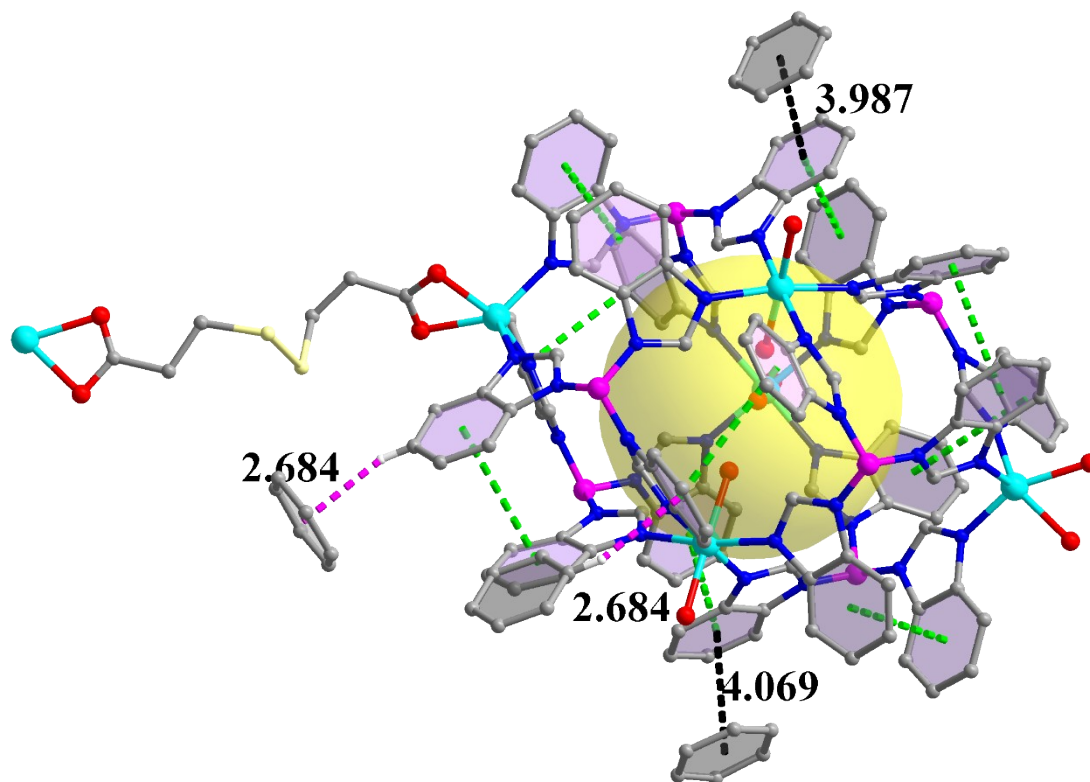


Figure S14. Intermolecular $\pi \cdots \pi$ interaction in BIF-139. (unit : Å).

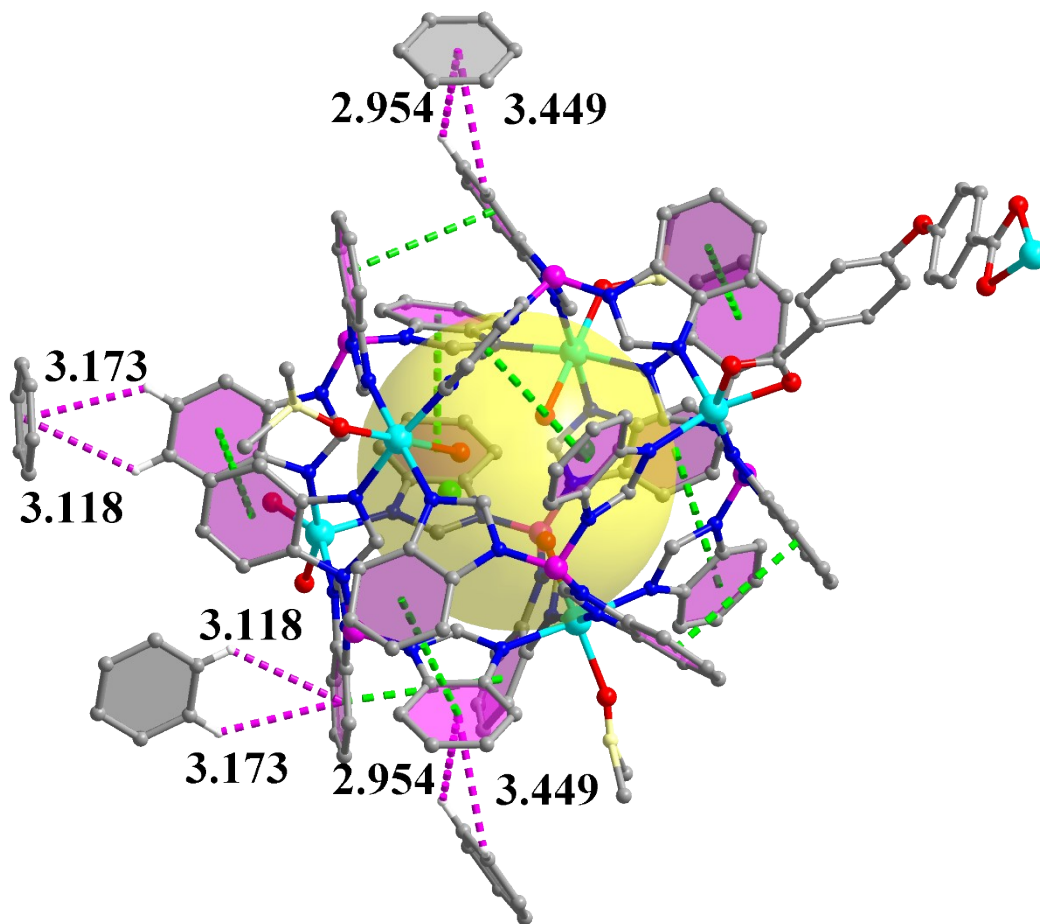


Figure S15. Intermolecular $\pi \cdots \pi$ interaction in BIF-137. (unit : Å).

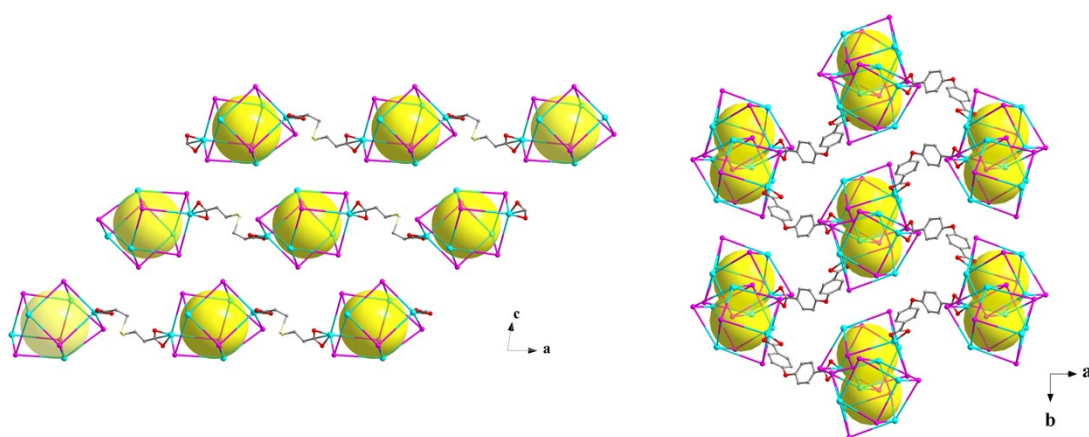


Figure S16. Stacking of BIF-139 (left) and BIF-137 (right).

3. The PXRD Analyses for BIFs

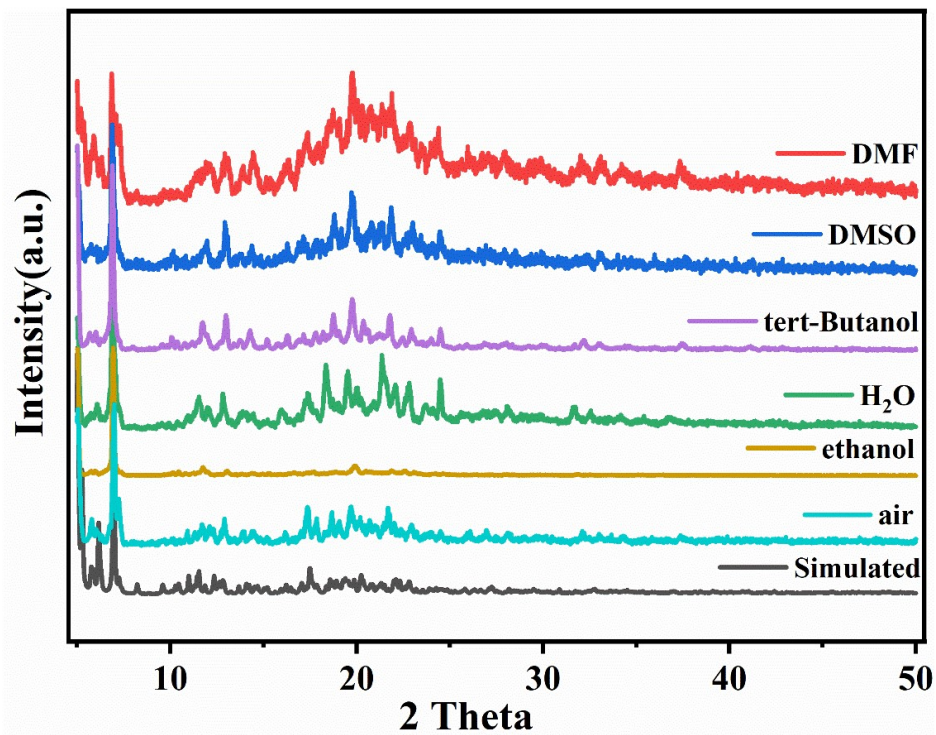


Figure S17. The PXRD patterns of BIF-136

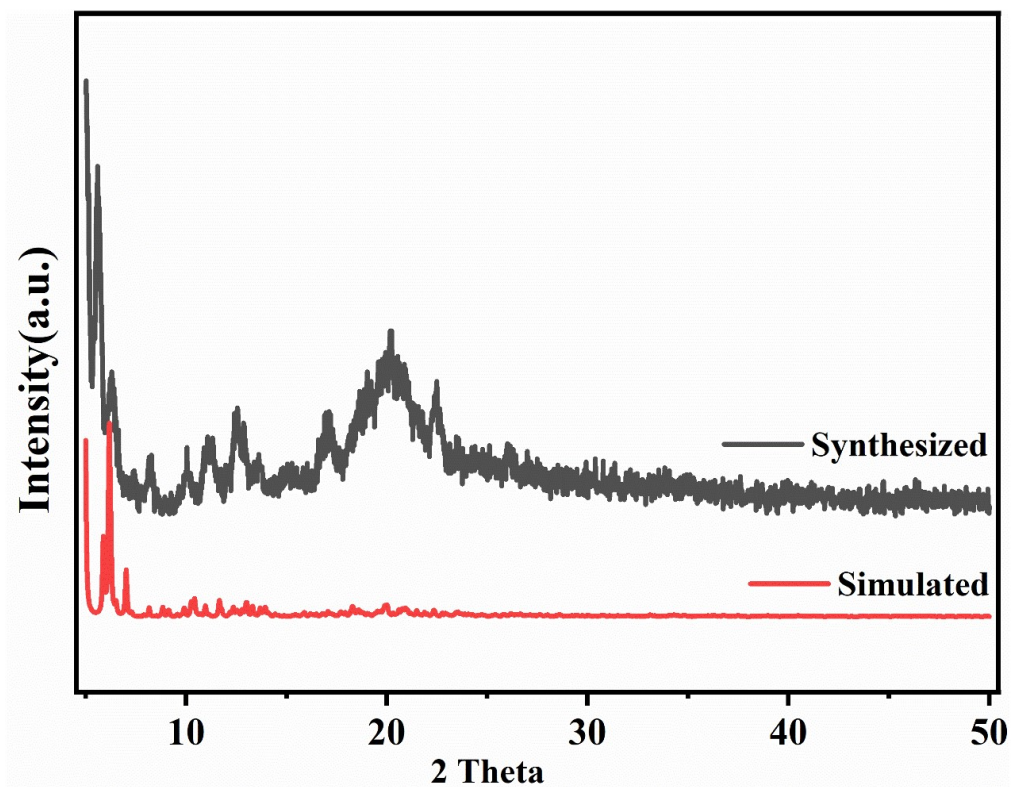


Figure S18. The PXRD patterns of BIF-137

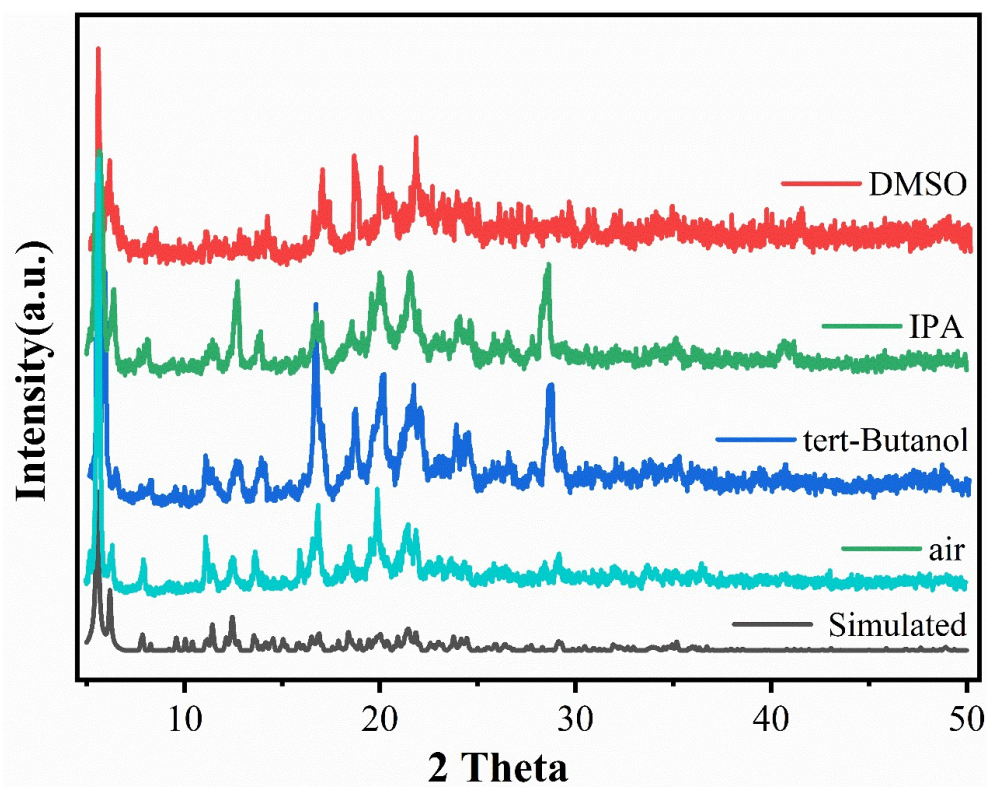


Figure S19. The PXR D patterns of BIF-138

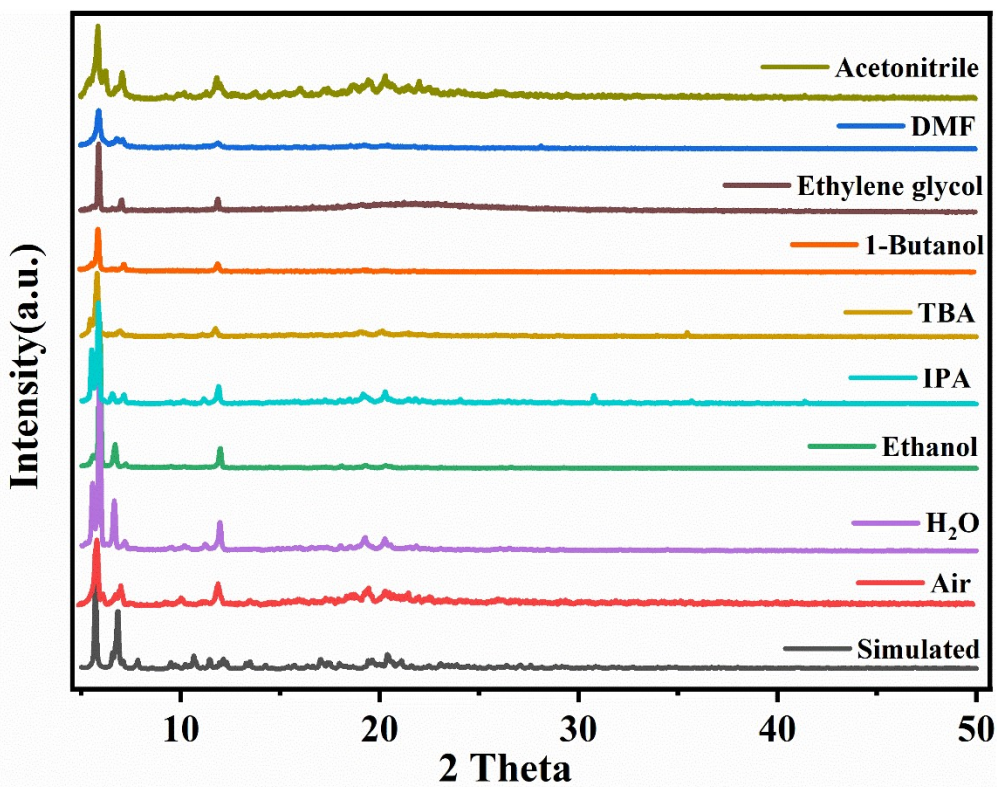


Figure S20. The PXR D patterns of BIF-139

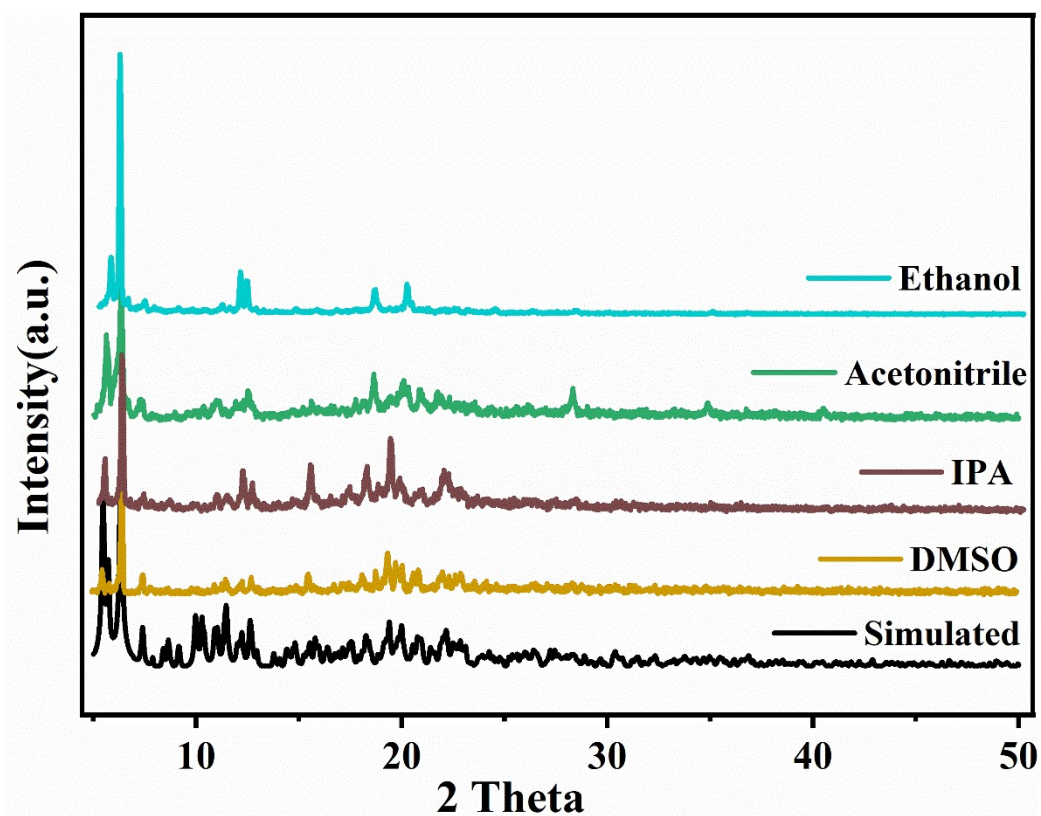


Figure S21. The PXRD patterns of BIF-140

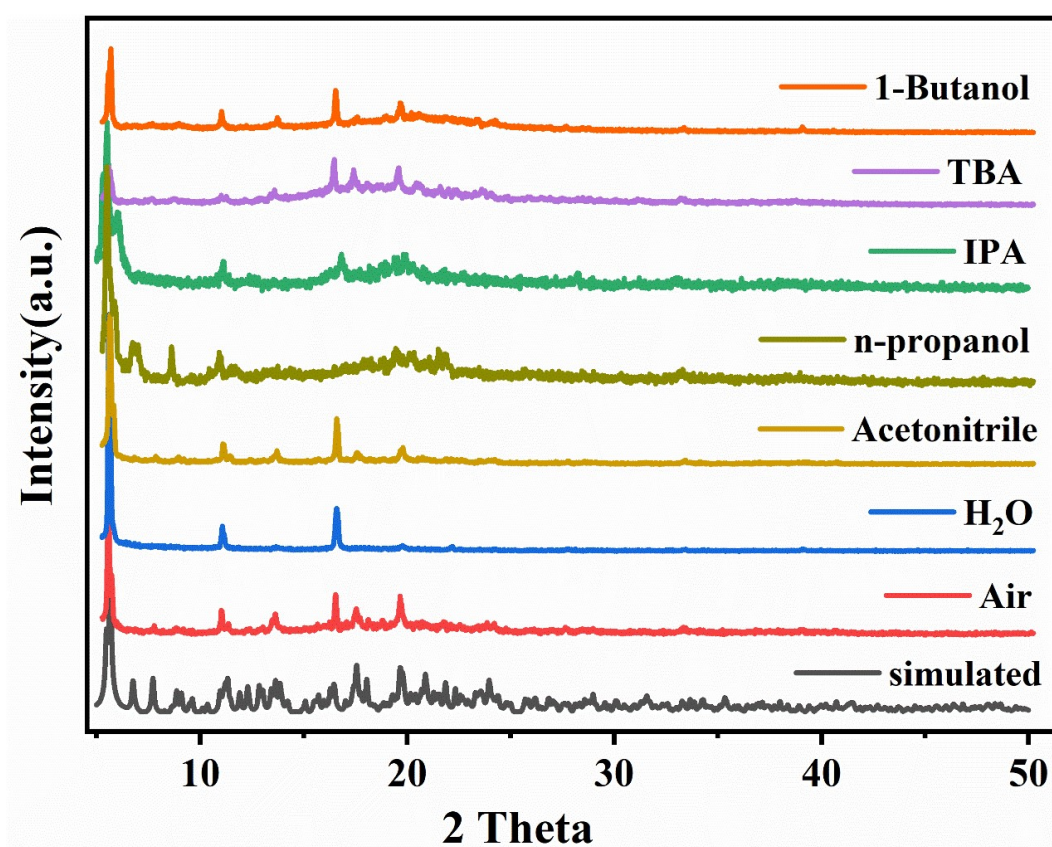


Figure S22. Solvent stability of BIF-141

4. The UV-Vis Spectra of BIFs

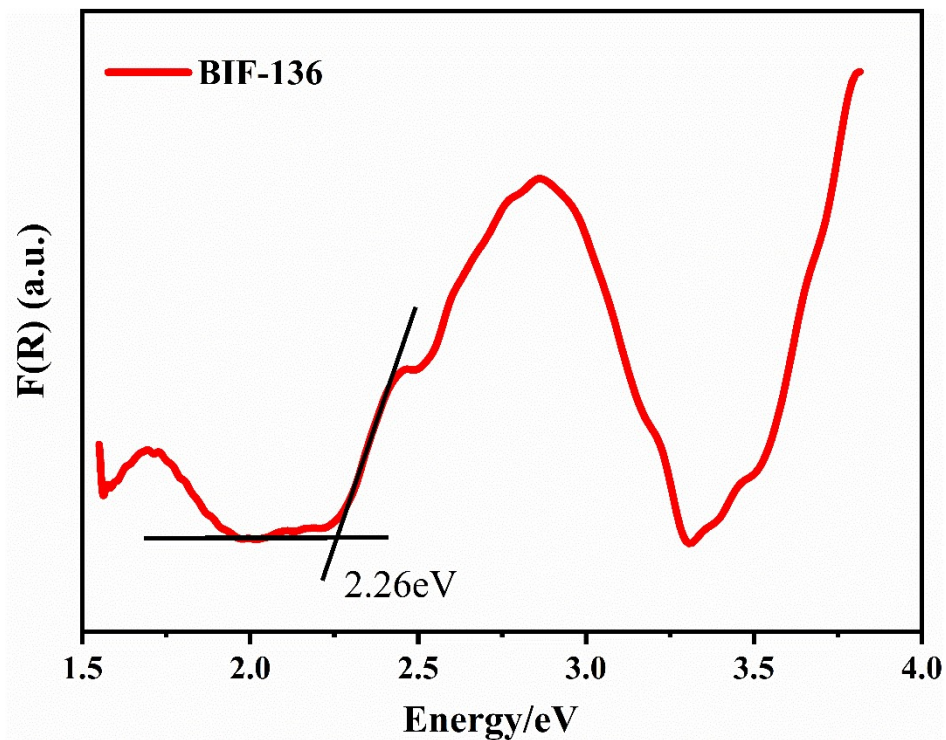


Figure S23. The band gap of BIF-136

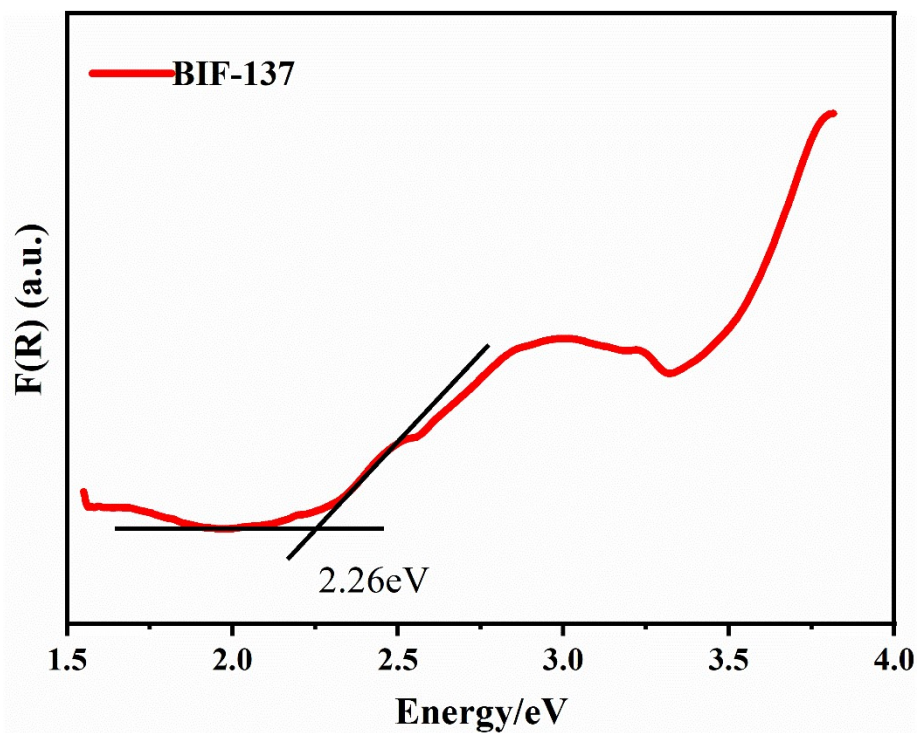


Figure S24. The band gap of BIF-137

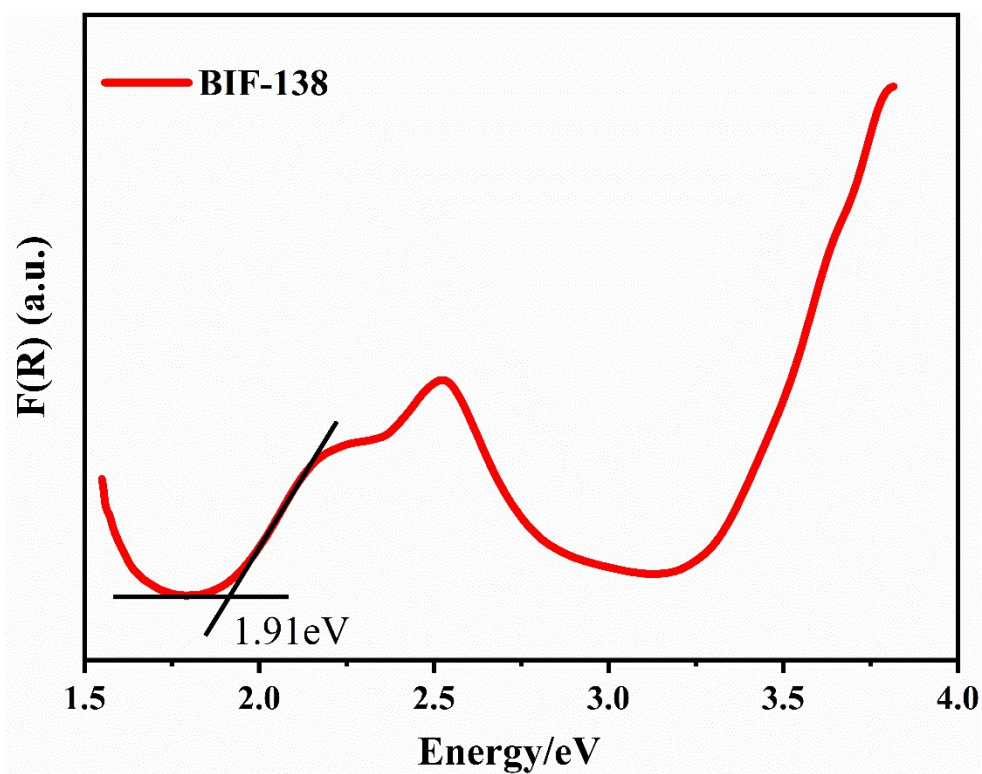


Figure S25. The band gap of BIF-138

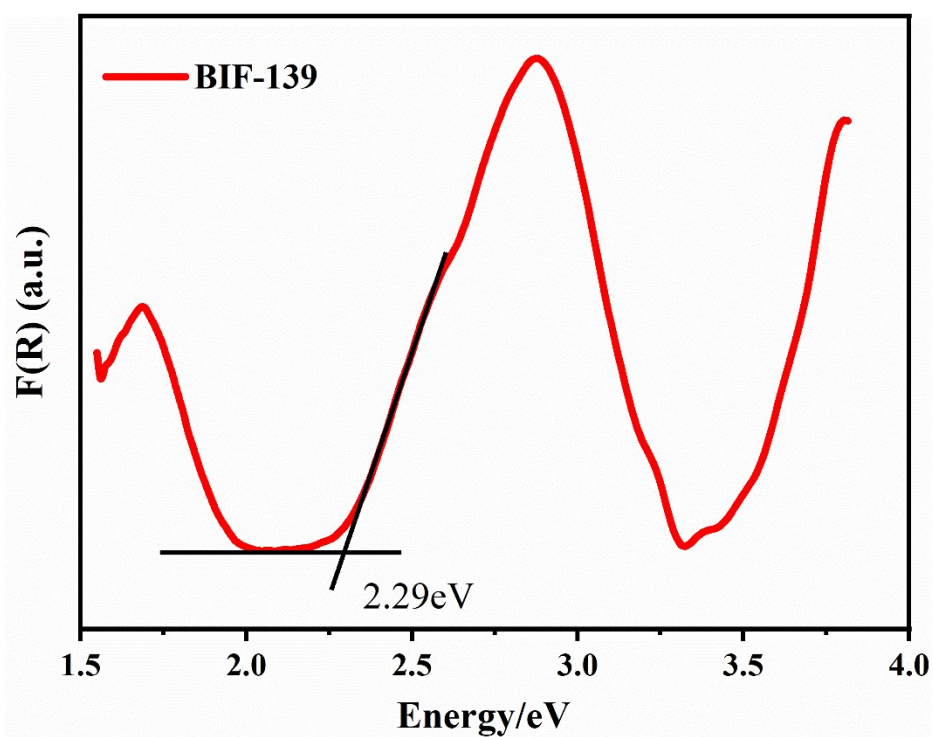


Figure S26. The band gap of BIF-139

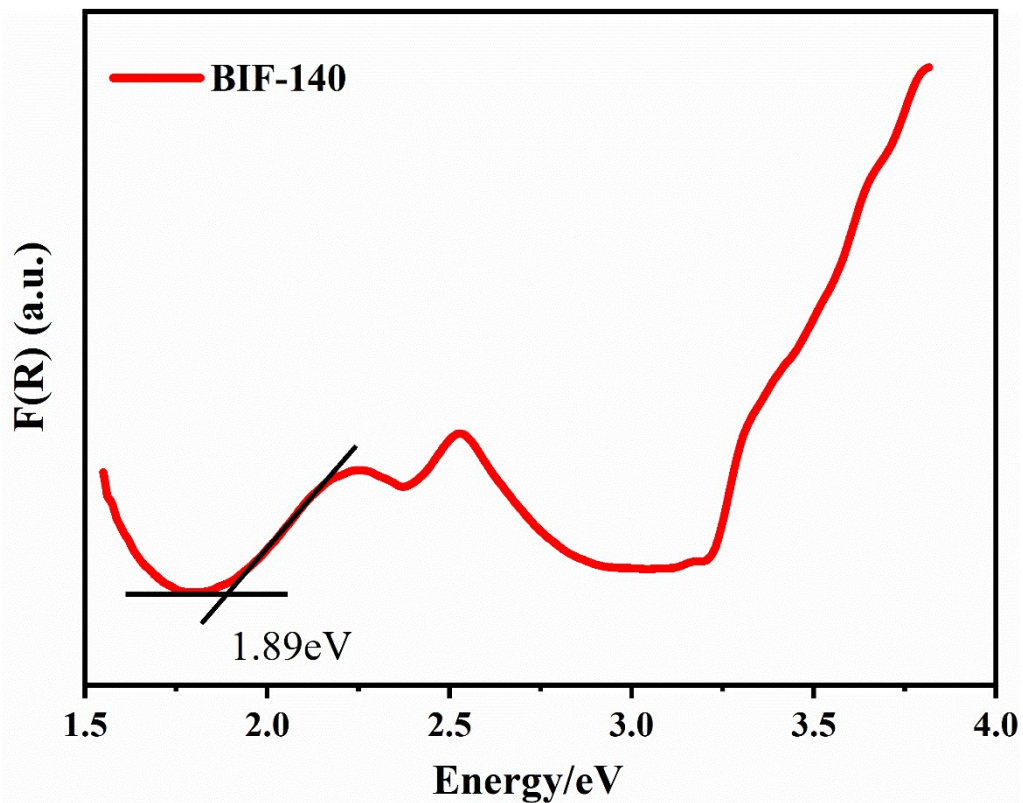


Figure S27. The band gap of BIF-140

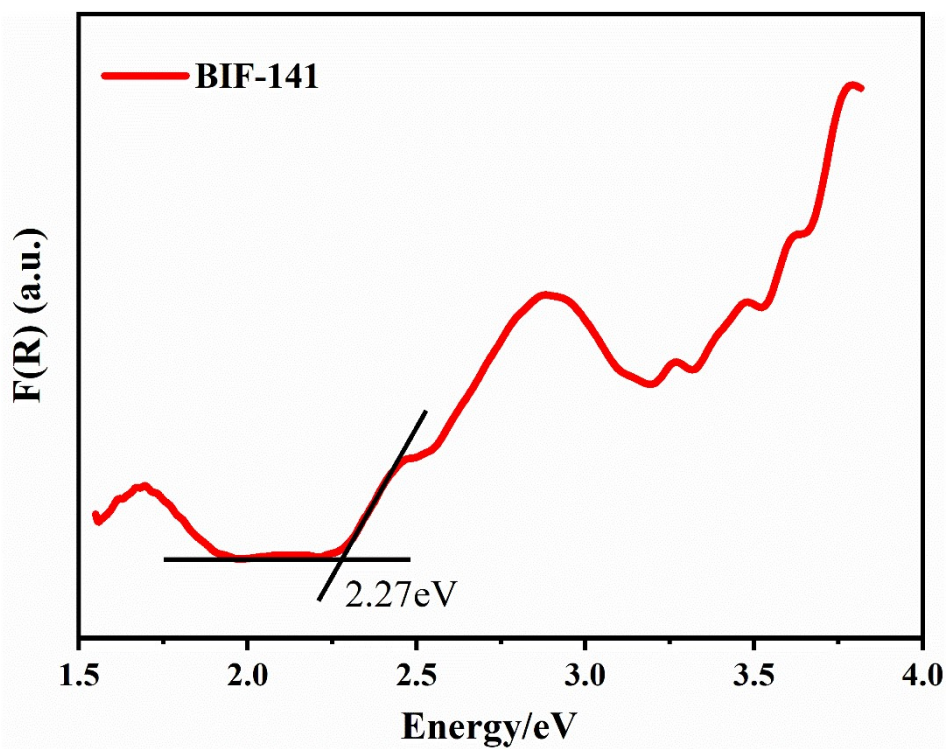


Figure S28. The band gap of BIF-141.

5. The NLO Property

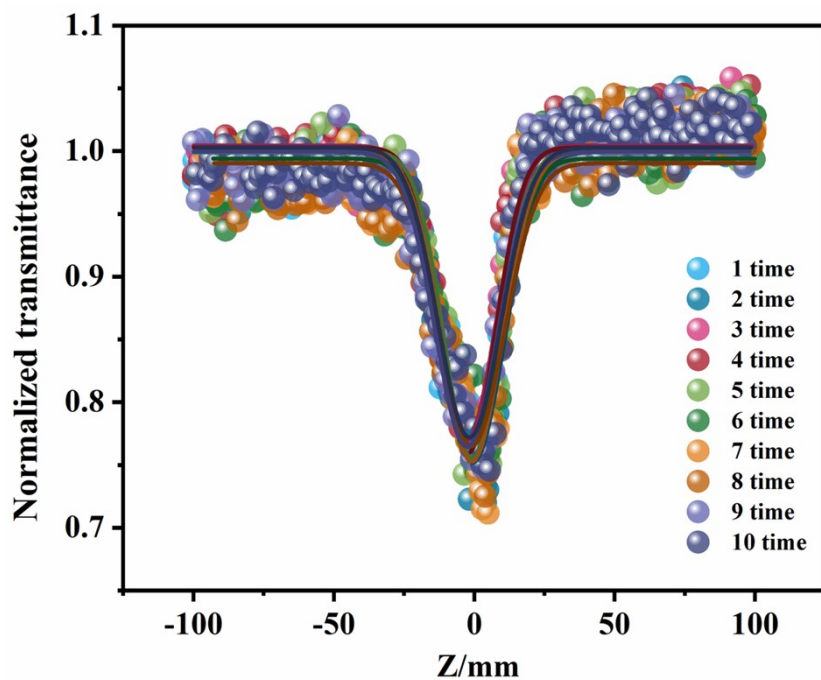


Figure S29. The opening Z-scan curve at 532 nm of BIF-136@PDMS.

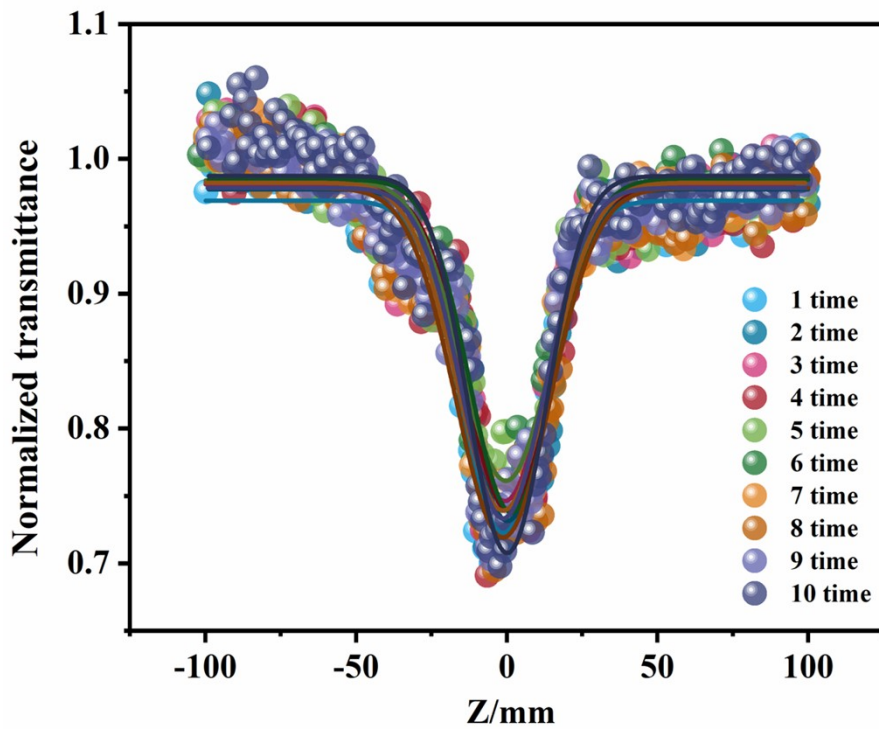


Figure S30. The opening Z-scan curve at 532 nm of BIF-137@PDMS.

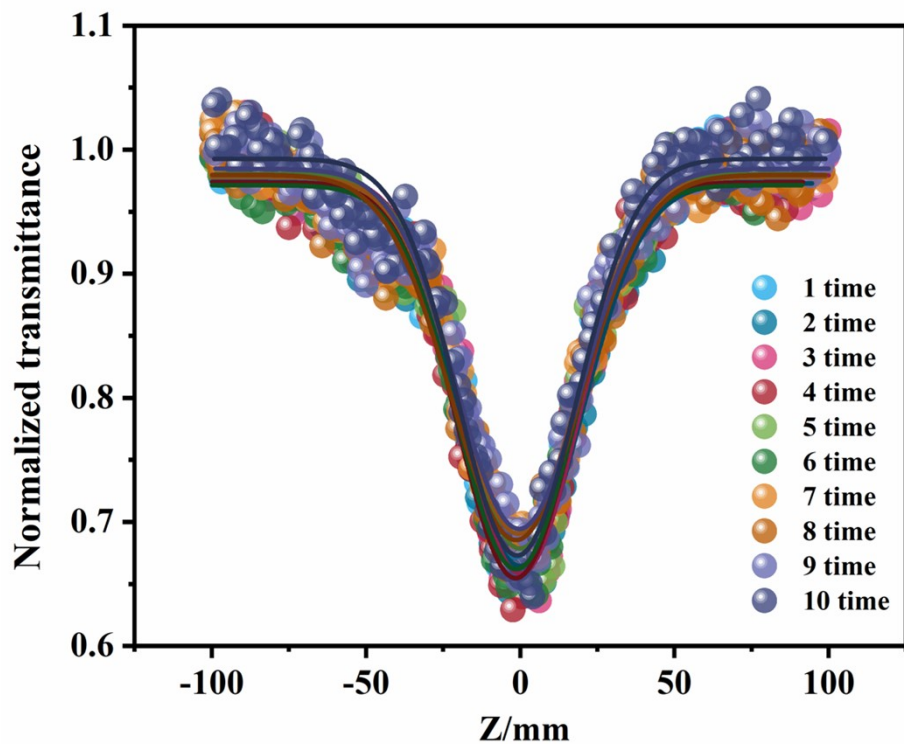


Figure S31. The opening Z-scan curve at 532 nm of BIF-138@PDMS.

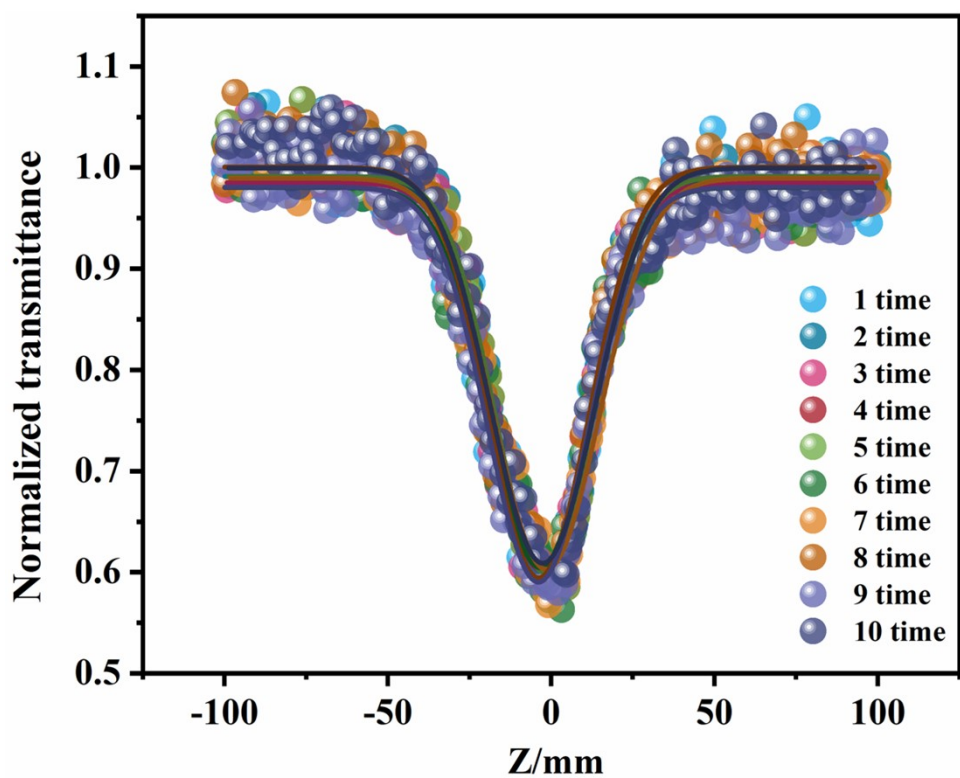


Figure S32. The opening Z-scan curve at 532 nm of BIF-139@PDMS.

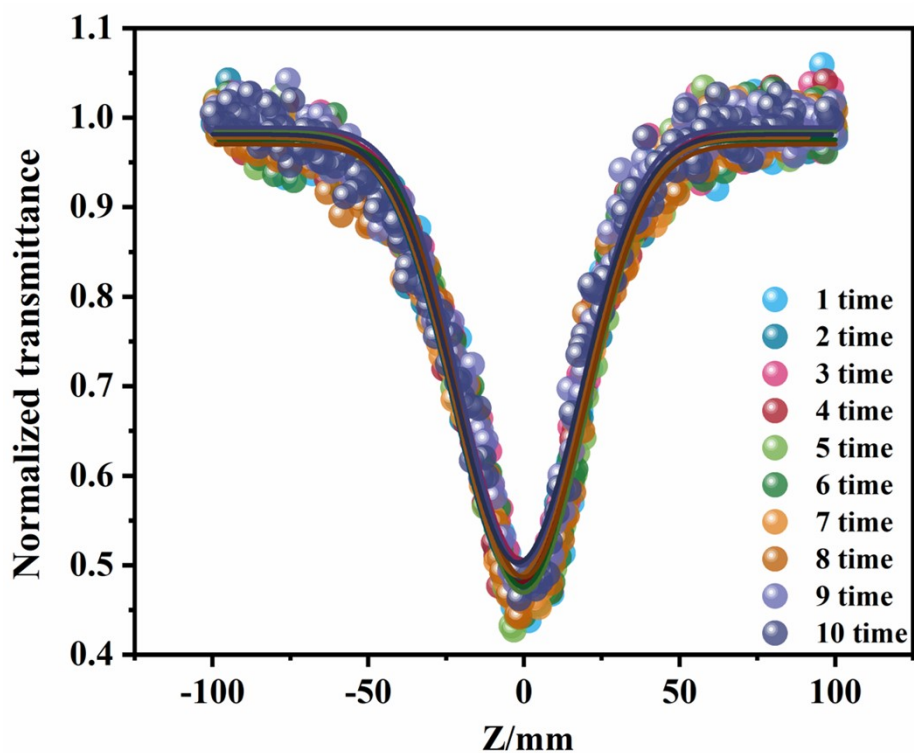


Figure S33. The opening Z-scan curve at 532 nm of BIF-140@PDMS.

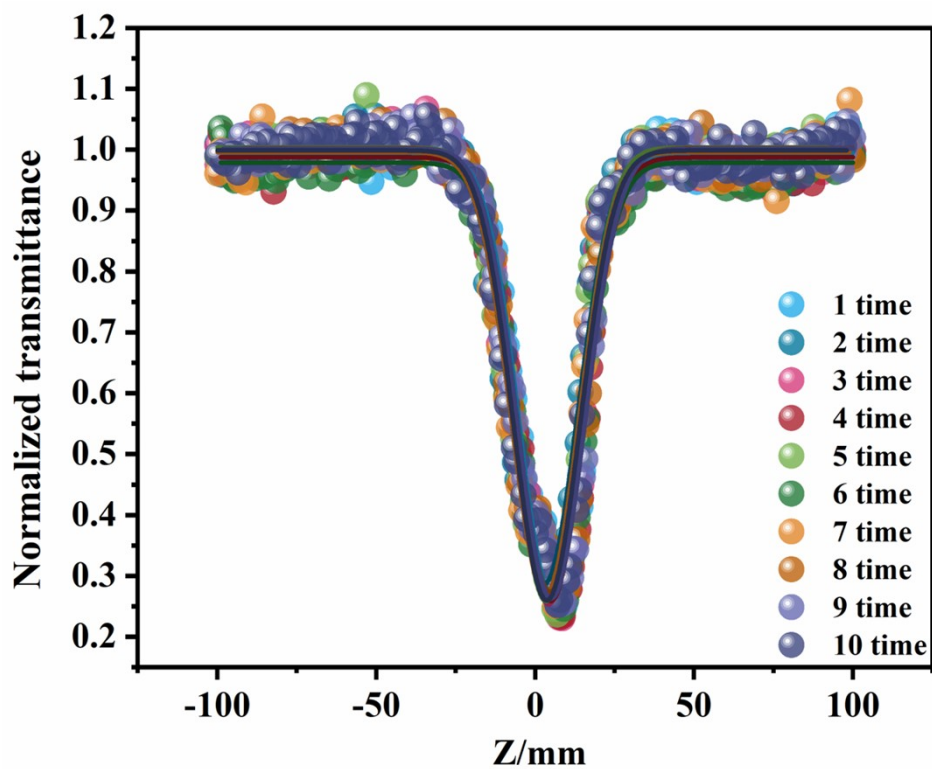


Figure S34. The opening Z-scan curve at 532 nm of BIF-141@PDMS.

Table S1. Linear transmittance (T%), the minimum normalized transmittance (T_{\min}), nonlinear absorption coefficient (β), imaginary part of third-order nonlinear susceptibility $Im\chi^{(3)}$ and Optical limiting threshold F_{OL} values of the samples

Sample	T (%)	T_{\min}	$\beta(\times 10^{-10}\text{m/W})$	$F_{OL}(\text{J/cm}^2)$	$Im\chi^{(3)}(\times 10^{-11}\text{esu})$
BIF-136@PDMS	75	0.765	4.8	17.4	1.02
BIF-137@PDMS	70	0.76	4.8	15.2	1.02
BIF-138@PDMS	73	0.68	7.8	3.42	1.65
BIF-139@PDMS	67	0.61	10.4	6.91	2.20
BIF-140@PDMS	70	0.50	19.5	1.95	4.13
BIF-141@PDMS	78	0.20	90.0	1.43	19.0

6. The TGA curve of BIFs

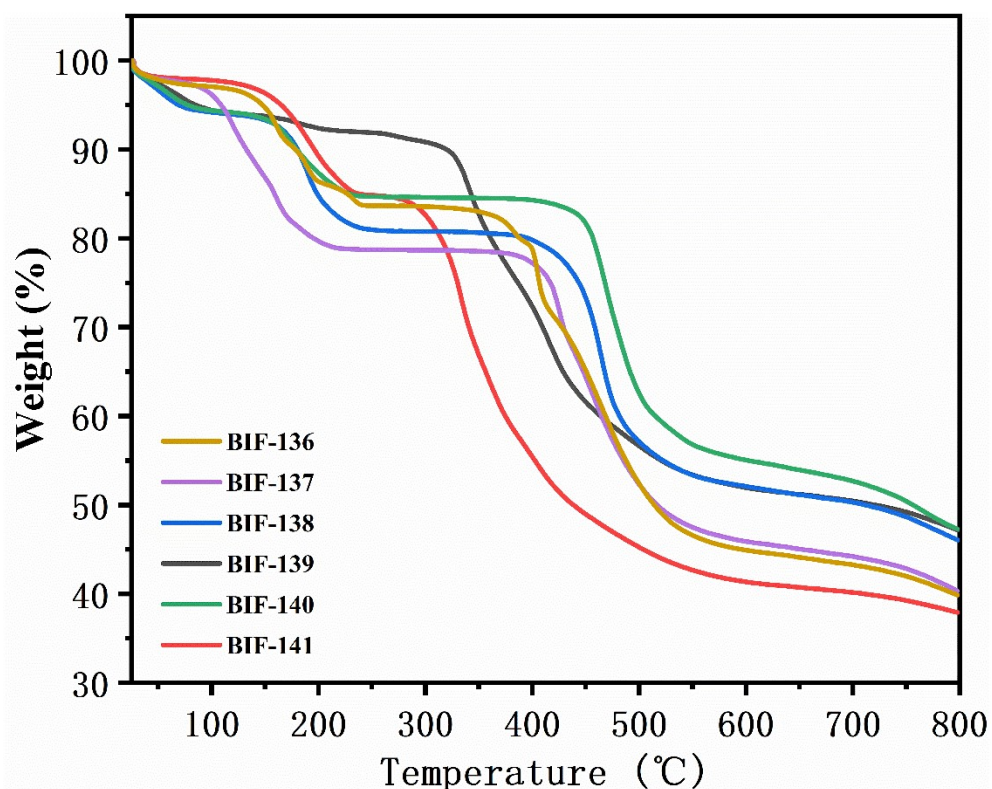


Figure S35. The TGA curve of BIFs

7. Crystallography Data

Table S2. Crystallographic Data and Structure Refinement Details for BIF-136 to BIF-141

	BIF-136	BIF-137	BIF-138
Formula	C ₁₆₂ H ₁₅₅ B ₆ Cl ₂ N ₃₉ Ni ₅ O ₁₅	C ₁₄₆ H ₁₀₉ B ₆ Cl ₂ N ₃₆ Ni ₅ O ₁₁ S ₃	C ₁₃₂ H ₁₂₀ B ₆ Cl ₄ N ₃₆ Ni ₅ O ₆ S ₃
Formula weight	3317.55	3069.18	2903.02
Temperature/K	100.01(10)	100	99.99(14)
Crystal system	triclinic	monoclinic	orthorhombic
Space group	<i>P</i> -1	<i>P</i> 2 ₁ / <i>n</i>	<i>P</i> na2 ₁
a/Å	18.7858(3)	30.3280(5)	22.68490(10)
b/Å	19.3734(4)	16.5538(2)	22.43500(10)
c/Å	26.4020(6)	37.8240(7)	31.61590(10)
α/°	74.342(2)	90	90
β/°	88.378(2)	109.405(2)	90
γ/°	70.434(2)	90	90
Volume/Å³	8697.6(3)	17910.6(5)	16090.46(11)
Z	2	4	4
ρ_{calc}/cm³	1.267	1.138	1.198
Reflections collected	126982	135747	199988
Independent reflections	34718 [R _{int} = 0.0832, R _{sigma} = 0.0828]	35925 [R _{int} = 0.0841, R _{sigma} = 0.0874]	32361 [R _{int} = 0.0539, R _{sigma} = 0.0366]
GOF on F²	1.021	1.040	1.020
Final R indexes [I ≥ 2σ(I)]	R ₁ = 0.0863, wR ₂ = 0.1847	R ₁ = 0.0899, wR ₂ = 0.2206	R ₁ = 0.0750, wR ₂ = 0.1934
Final R indexes [all data]	R ₁ = 0.1279, wR ₂ = 0.2056	R ₁ = 0.1599, wR ₂ = 0.2580	R ₁ = 0.0870, wR ₂ = 0.2023

(Continued) Table S2. Crystallographic Data and Structure Refinement Details for BIF-136 to BIF-141

	BIF-139	BIF-140	BIF-141
Formula	C ₁₄₇ H ₁₄₇ B ₆ Cl ₂ N ₃₉ Ni ₅ O ₁₅ S ₂	C ₁₃₅ H ₁₂₅ B ₆ Cl ₄ N ₃₈ Ni ₅ O ₇ S	C ₁₅₆ H ₁₇₅ B ₆ Cl ₂ N ₄₀ Ni ₅ O ₁₆ S ₄
Formula weight	3193.46	2923.98	3424.91
Temperature/K	100.02(10)	100.00(10)	100.00(10)
Crystal system	triclinic	monoclinic	monoclinic
Space group	<i>P</i> -1	<i>I</i> 2/a	<i>C</i> 2/ <i>c</i>
a/Å	18.4610(2)	30.6994(6)	33.8501(3)
b/Å	18.8062(2)	32.1537(6)	22.8948(2)
c/Å	23.1024(3)	35.2206(8)	22.8811(3)
α/°	81.9090(10)	90	90
β/°	80.5360(10)	114.260(2)	108.0090(10)
γ/°	89.4630(10)	90	90
Volume/Å³	7832.02(16)	31696.0(12)	16863.9(3)
Z	2	8	4
ρ_{calc}/cm³	1.354	1.225	1.349
Reflections collected	112316	117067	57896
Independent reflections	31503 [R _{int} = 0.0457, R _{sigma} = 0.0432]	31666 [R _{int} = 0.0855, R _{sigma} = 0.0833]	16591 [R _{int} = 0.0675, R _{sigma} = 0.0548]
GOF on F²	1.031	1.018	1.028
Final R indexes [I ≥ 2σ(I)]	R ₁ = 0.0774, wR ₂ = 0.1890	R ₁ = 0.0901, wR ₂ = 0.2207	R ₁ = 0.0963, wR ₂ = 0.2338
Final R indexes [all data]	R ₁ = 0.1100, wR ₂ = 0.2160	R ₁ = 0.1370, wR ₂ = 0.2519	R ₁ = 0.1258, wR ₂ = 0.2563

8. PDMS film forming method and Test methods for third-order NLO

First, 10mg of sample was mixed with 3g PDMS, and the sample was evenly dispersed by magnetic stirring for several hours. The second step is to add 1/10 mass of specific curing agent and continue to stir evenly for about 10min. The third step is to take 1g of the mixture and put it into a specific membrane. Under the action of gravity, the mixture is paved in the mold, and placed at room temperature for about half an hour to eliminate bubbles. Finally, put the membrane utensil into a 60 °C oven for 5h to obtain samples for testing.

Z-scan measurements

The output fluence versus input fluence of the sample can be measured by opening Z-scan curve. The OL curve in the figure 3-d can be calculated from the laser input pulse energy and the spot radius $w(z)$:

the light fluence $F_{in}(z)$ at any position is defined as:

$$F_{in}(z) = \frac{4E_{in}\sqrt{\ln 2}}{3\pi^2\omega_{(z)}^2}$$

where $\omega(z)$ is defined as:

$$\omega_{(z)} = \omega_0 \left[1 + \left(\frac{z}{z_0} \right)^2 \right]^{\frac{1}{2}}$$

where ω_0 and z_0 are the light beam radius and the Rayleigh range, respectively, and z_0 is defined as:

$$z_0 = \frac{k\omega_0^2}{2}$$

where k is defined as:

$$k = \frac{2 \times \pi}{\lambda}$$

In addition, the imaginary part of the third-order nonlinear polarizability is calculated by the following formula :

$$\text{Im } \chi^{(3)}(esu) = \frac{\lambda \varepsilon_0 c^2 n_0^2}{4\pi^2} \beta(m/w)$$